NASA TECHNICAL NOTE

NASA TN D-4259

BALLISTIC LIMIT OF ALUMINUM PLATES DETERMINED BY AN EXPLODING FOIL GUN TECHNIQUE

by Emilio Alfaro-Bou and Robert G. Thomson

Langley Research Center
Langley Station, Hampton, Va.

NATIONAL AERONAUTICS AND SPACE ADMINISTRATION • WASHINGTON, D. C. • DECEMBER 1967

BALLISTIC LIMIT OF ALUMINUM PLATES DETERMINED BY AN EXPLODING FOIL GUN TECHNIQUE

By Emilio Alfaro-Bou and Robert G. Thomson

Langley Research Center
Langley Station, Hampton, Va.

NATIONAL AERONAUTICS AND SPACE ADMINISTRATION

For sale by the Clearinghouse for Federal Scientific and Technical Information
Springfield, Virginia 22151 – CFSTI price $3.00

BALLISTIC LIMIT OF ALUMINUM PLATES DETERMINED BY AN EXPLODING FOIL GUN TECHNIQUE

By Emilio Alfaro-Bou and Robert G. Thomson
Langley Research Center

SUMMARY

An understanding of the perforation of finite-thickness plates is essential to the proper design of spacecraft to insure protection from meteoroid impact. An investigation was therefore initiated to determine the ballistic limits of finite-thickness plates and to compare these results with existing theoretical predictions. The impact of meteoroids on thin aluminum plates is simulated in an exploding foil gun facility. The exploding foil gun can fire a large number of shots in a relatively short time with a range of projectile velocities from 1 to 8 km/s. The exploding foil gun facility is used in an experimental program to determine the ballistic limits of aluminum plates of varying thickness. The information gathered from this experimental program indicates that the ballistic limit is linearly dependent on the plate thickness and the experimental data correlate well with the theory of ballistic limit developed from a visco-plastic model. Hence, the current practice of using semi-infinite penetration data in predicting the ballistic limits of thin plates is incorrect.

INTRODUCTION

The impingement and penetration of the main wall of a space vehicle by meteoroids is of major concern to the spacecraft designer. To design adequately for spacecraft protection, it is necessary to understand the relation between perforation of thin-wall structures and impact velocity. The ballistic limit properties of thin-wall structures are the specific concern of the present paper.

The term "ballistic limit" is herein defined as that velocity at which a projectile would just perforate a given target. A criterion used by many investigators for predicting ballistic limits is to multiply the crater depth in a semi-infinite target by a numerical factor ranging in value from 1 to 2.5. This product, presumably, is the thickness of a single plate that is just perforated by the projectile that caused the crater in the semi-infinite media. The assumption tacitly accepted in adopting this criterion is

that the perforation of thin sheets and the penetration into semi-infinite solids are essentially the same physical mechanism. It has been shown by many investigators (for example, refs. 1 and 2) that, in semi-infinite solids, the crater depth is dependent on the projectile velocity raised to the two-thirds power. Thus, the velocity dependence for the perforation of thin plates, using the semi-infinite criterion, must also be described by the velocity raised to the two-thirds power.

The ballistic limit of thin plates has been determined in reference 3 by directly analyzing the behavior of the impacted plate. This analysis considers the thin plate to be a visco-plastic continuum in which the impacting projectile is assumed to shear out a plug of the sheet material in the process of perforation. The thickness at the ballistic limit, as determined from reference 3, indicates a linear relationship between plate thickness and projectile velocity.

An experimental program to investigate the velocity exponent of the ballistic limit plate-thickness dependence was, therefore, initiated for finite plates. The results of the program with a full description of the experimental techniques employed are reported herein.

Ballistic limit determination is costly and time consuming because it requires a large number of experimental shots before a valid data point is established. The exploding foil gun facility, however, is particularly adaptable to this type of study because the gun can fire a large number of shots in a relatively short time with the cost per shot being comparatively nominal. Also, projectile velocities obtainable are quite flexible, ranging in this experimental program from 1 to 8 km/s for projectile masses of 10 and 30 mg.

The units for the physical quantities used in this paper are given in the International System of Units (SI). The relationship between this system and U.S. Customary Units is given in reference 4.

DESCRIPTION OF FACILITY

The exploding foil gun facility used in this program at the Langley Research Center is simple and compact. (See fig. 1.) It consists of a 70-kV power supply, a high-voltage capacitor bank, a spark-gap switch, an expendable foil gun, and an evacuated test chamber containing the target. The facility also contains a projectile time-displacement measuring system consisting of three cameras and three flash lamps as shown in figure 2.

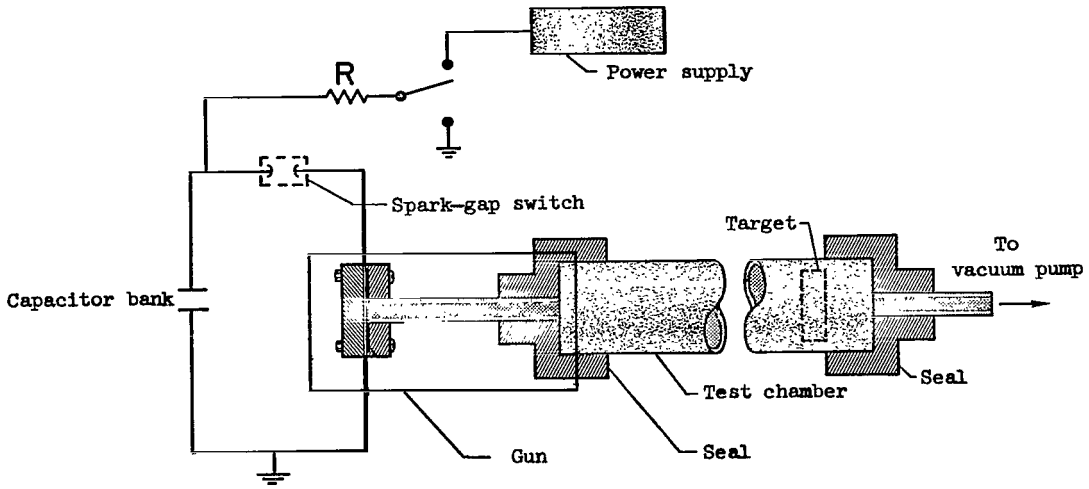

Figure 1.- Schematic of exploding foil gun facility.

Exploding Foil Gun

The guns used in the experiments of this report were made of plexiglass. Each gun is usable for only one shot because it disintegrates after firing. The gun consists of a breechblock, aluminum foil, connecting leads, diaphragm, and barrel assembly (fig. 3). The 5- by 5- by 1.25-cm breechblock serves as an inertia block to help contain the pressure generated in the explosion of the aluminum foil. The foil is 2.5 cm long; the foil thickness is dependent on the energy stored in the capacitors and varies from 12.5 to 38 μm. The thinner material was used in the lower velocity shots. The exploding foil produces a pressure pulse which shears a disk-like projectile from the diaphragm. The diaphragm is made of 0.25-mm-thick plastic film (ref. 5) for the 6.4-mm-diameter projectile and of 0.36-mm-thick plastic film for the 9.5-mm-diameter projectile. Besides providing the projectile, the diaphragm also serves as a vacuum seal between the chamber and the gun breech. The connecting leads are made of folded aluminum, are 0.25 mm thick, and connect the foil between ground and one electrode of the firing switch.

The barrel assembly is similar to the breechblock except that a 102-mm-long plexiglass tube is inserted through a hole in the center of the block's larger face. The projectile is a disk formed by shearing action which occurs from the pressure differential between the diaphragm and the tube in the barrel assembly. A 6.4-mm-inside-diameter barrel provides a 6.4-mm-diameter disk. The relatively long barrel guides the projectile with reasonable accuracy into the target. The barrel also provides a quick method of attaching the gun to the vacuum chamber through a rubber seal. Further discussion of this exploding foil gun technique can be found in reference 6.

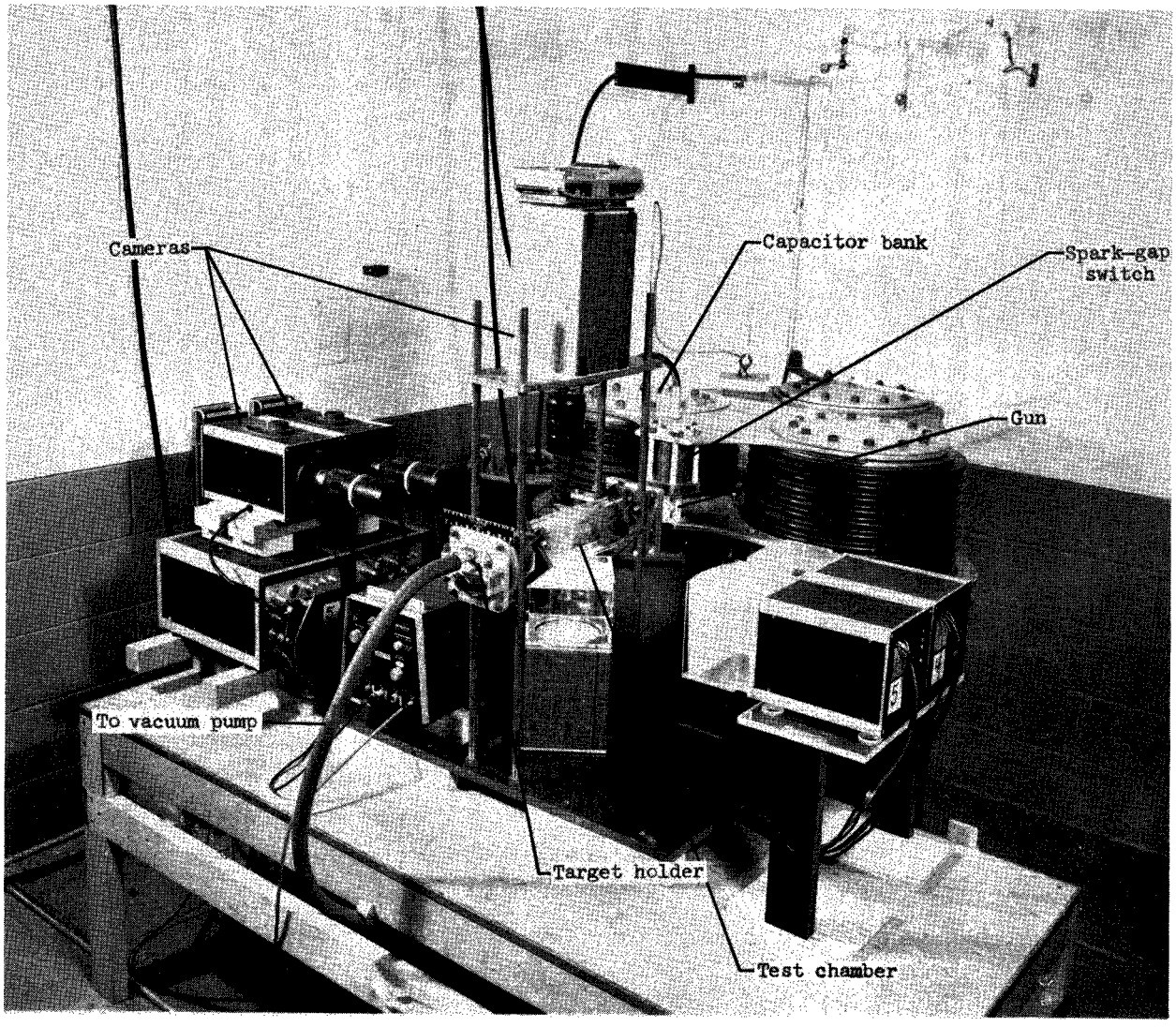

(a) General view. L-67-6653

Figure 2.- Exploding foil gun facility. (Note that projectile travels from right to left.)

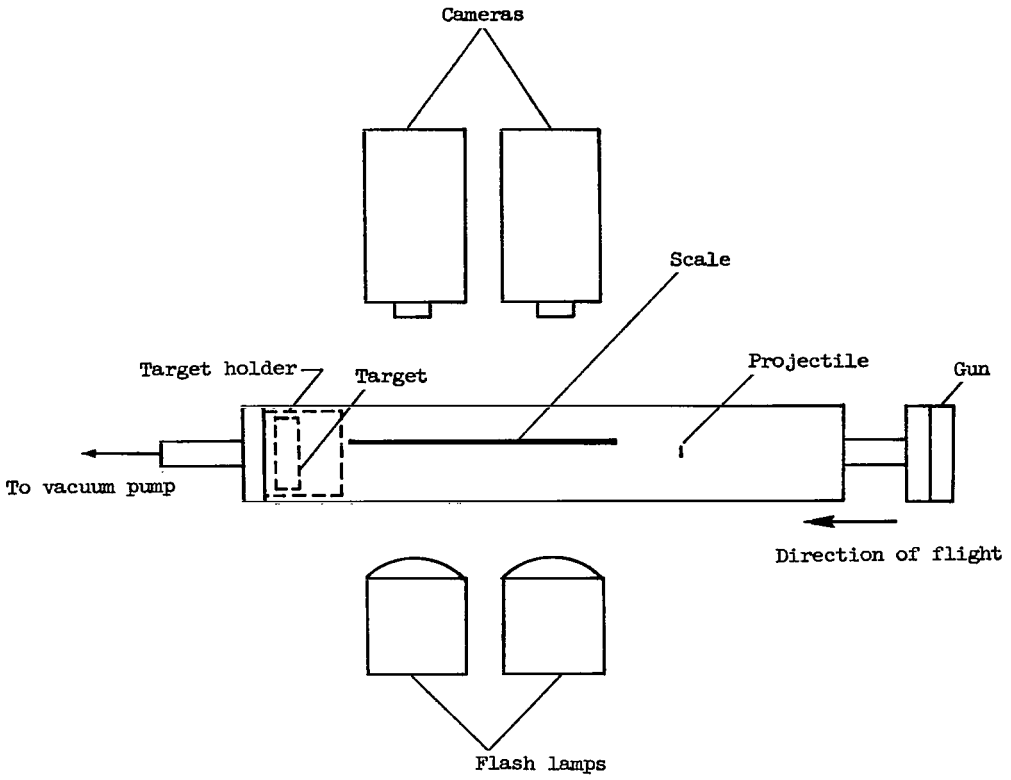

(b) Closeup schematic.

Figure 2.- Concluded.

Test Chamber

The test chamber is a thick-wall glass pipe, 7.6 cm inside diameter and 45.7 cm long. (See fig. 2(b).) The chamber can be pumped down to a vacuum of 1 N/m^2 (10^{-2} mm Hg), 5 N/m^2 being the normal operating vacuum. A translucent scale is placed on the chamber to reference the location of the projectile when photographed anywhere within the chamber. Two orthogonal pictures of the projectile can be taken simultaneously to determine the orientation of the projectile near the target and its integrity in flight prior to impact.

A target holder is clamped to one end of the glass chamber. The holder is a 13-cm-long hollow metal cylinder with a vacuum connection in the flat capped end. The target is inserted in the holder between two spacer rings that clamp the outer edge of the target uniformly. A retaining ring is inserted against the outer ring to hold the assembly in place. (See fig. 4.) A backplate is used to protect the holder from target and projectile fragments.

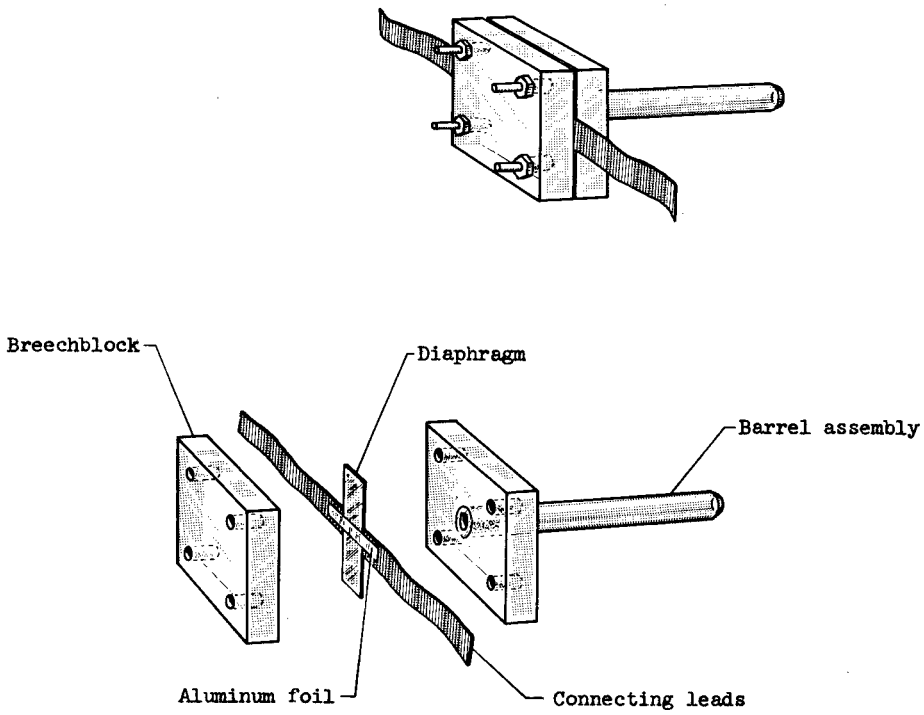

Figure 3.- Exploding foil gun.

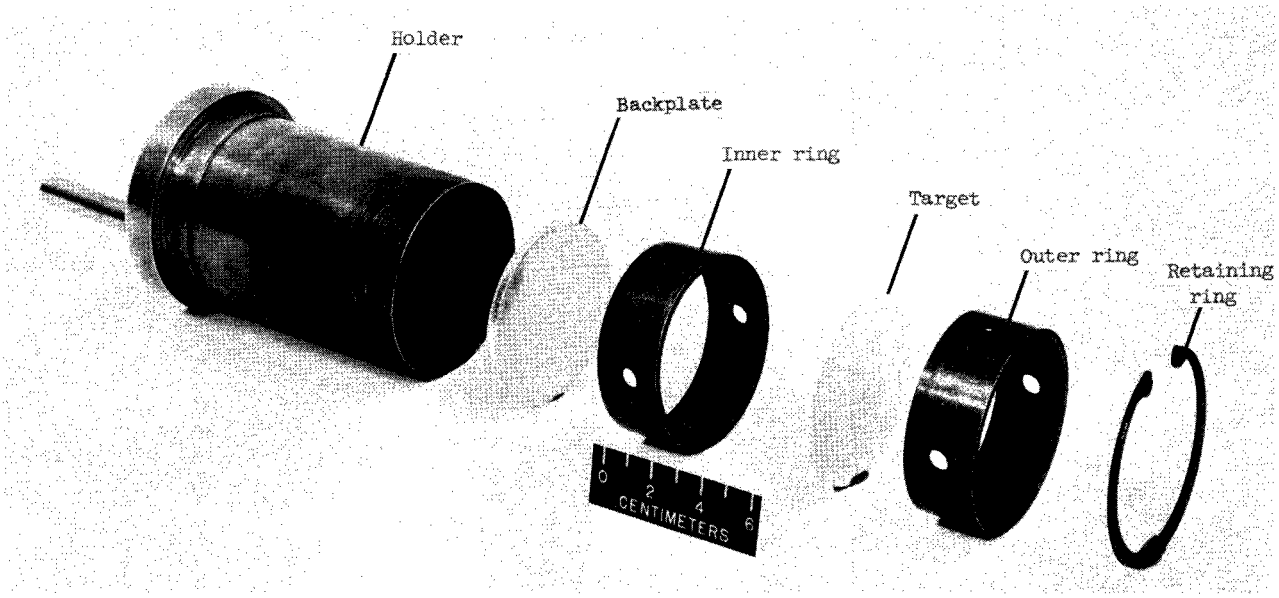

Figure 4.- Target holder.

L-67-6654

Spark-Gap Switch

The pressurized spark-gap switch for the capacitor bank consists of two copper electrodes separated by an air gap, the air acting as a dielectric. The gap in the switch is adjustable such that a range of voltages from 5 to 70 kV can be triggered, 70 kV being the maximum power supply voltage. One electrode of the switch is connected to the high voltage plate of the capacitor bank. The other electrode is connected to one of the gun leads. The switch is triggered by reducing the air pressure; this allows the capacitors to be discharged through the switch and the gun.

Power Supply and Capacitor Bank

The dc high voltage power supply has the capability of delivering a maximum of 70 kV at a charging rate of 30 mA. The high voltage side is connected to the top plate of the capacitor bank. The bank consists of from one to five capacitors connected in parallel, depending on the amount of energy desired. Each capacitor has an inductance of 80 nH and a capacitance of 1 μF and can accept a maximum charging voltage of 120 kV. An automatic safety switch is connected between the lower plate (ground plate) and the top plate of the bank to ground any residual charge in the capacitors after they have been fired.

Velocity Determination

The velocity was obtained by measuring the projectile's displacement during flight. Image converter cameras were used to photograph the projectile in flight. The shutter speeds of these cameras can be varied from 5 to 1000 ns; a speed of 50 ns was used in the present investigation. The cameras have a built-in delay that controls the triggering of the shutter from 1 to 100 μs after an initial signal is applied to the cameras. A longer delay can be obtained by utilizing a time-delay generator that further extends triggering of the shutter to 10 ms. The initial signal is obtained from the induced voltage generated by a coil located within the magnetic field of the capacitor bank discharge circuit. The time at which the camera shutter triggers is monitored by an oscilloscope. Directly opposite the cameras is a xenon filled flash lamp fully synchronized with the camera shutters to provide back lighting. The glass test chamber is located between the cameras and the flash lamps to permit photographing of the projectile in flight. Attached to the glass chamber is a scale to measure the projectile displacement.

The time intervals between exposures of the two cameras are set individually to photograph the projectile within the established velocity range for each shot. The velocity is first estimated from a predetermined voltage-velocity curve for that particular capacitor bank.

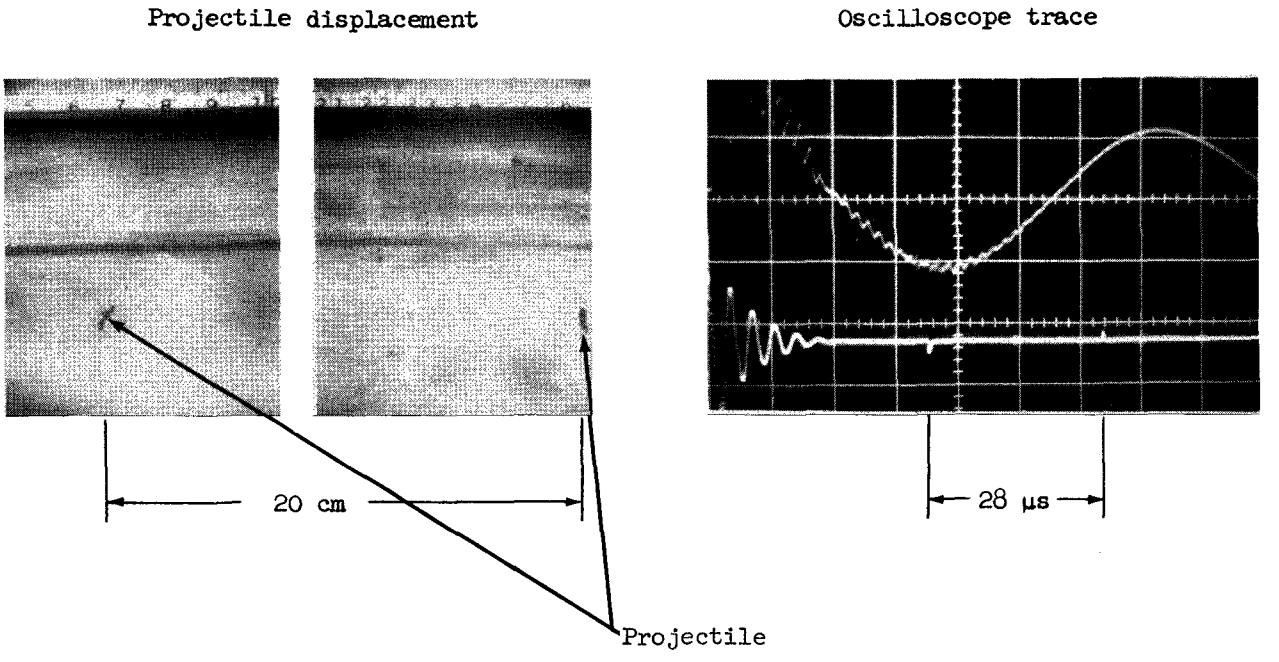

For impulse-type acceleration:

$$\text{Velocity} = \frac{\text{Displacement}}{\text{Elapsed time}} = \frac{20 \times 10^{-5}}{28 \times 10^{-6}} = 7.1 \text{ km/s}$$

Figure 5.- Velocity calculation. L-67-6655

The projectile velocity is calculated from the photograph of the projectile's displacement obtained by two parallel cameras and the elapsed time obtained from the oscilloscope trace which monitors the operation of the camera shutters. (See fig. 5.) An impulse-type acceleration of the plastic disk is assumed to occur at the moment of firing. The velocity is therefore assumed constant after leaving the gun barrel. This assumption of constant velocity has been verified by taking three consecutive photographs of the projectile in flight. The velocities calculated from these three projectile displacements indicated that the velocity did, indeed, remain constant within the error of the velocity measuring system (±5 percent).

In addition, the projectile's integrity and orientation can be determined from the photographs. This information, in conjunction with target impact examination, was used in determining an acceptable mode of projectile impact.

RESULTS AND DISCUSSION

Experimental Data

Single sheet 2024-T3 aluminum-alloy targets varying in thickness from 0.5 to 6.5 mm were used to obtain ballistic limit data for projectile velocities ranging from 1 to 8 km/s and projectile masses of 10 and 30 mg. The two different masses were obtained by varying the inside diameter of the gun barrel and the thickness of the diaphragm. Test results are given in table I and are plotted in figures 6 and 7.

The ballistic limit was determined by varying the projectile velocity V until the sheet is just perforated. The criterion for the ballistic limit was established by applying a penetrant dye to the impacted side of the target surface. A trace of the penetrant in the opposite face indicated a ballistic limit. A perforation or hole in the target indicated that the velocity was higher than the ballistic limit, and the absence of dye in the opposite face indicated that the velocity was too low.

A nominal value of the projectile mass was determined by weighing the initial mass of the undeformed projectile and decreasing this value by 10 percent. This nominal value of 90 percent of the initial projectile mass was arrived at from limited data obtained from a pendulum-type mass measurement device. The loss of projectile mass from launch to impact, as determined from the pendulum mass measurements, could be as high as 25 percent of the initial mass in some specific firings but, in general, amounted to only 10 percent.

The orientation of the disk prior to impact was determined from photographs taken by three cameras: an overhead camera and two side velocity-measuring cameras (fig. 2). These photographs, as well as indicating the type of damage done to the target plates, were used as criteria in determining the acceptability of each impact. Shown in figure 8 are photographs of the projectile in flight (from an overhead camera and a side camera) and of the target plates. Only a normal impact (flat impact), as in figure 8(a), was considered acceptable to correlate the results of this experimental program with the analytical treatment of reference 3. An unacceptable oblique impact is shown in figure 8(b) in which the projectile is seen to impact the target plate on edge. It was noted during the experimental program that oblique impacts were always more damaging than normal impacts and would exhibit lower ballistic limits. In figure 8(c) the integrity of the projectile during flight is seen to be lost, with a resultant excessive fragmentation of the projectile before impact; this type of impact also is unacceptable.

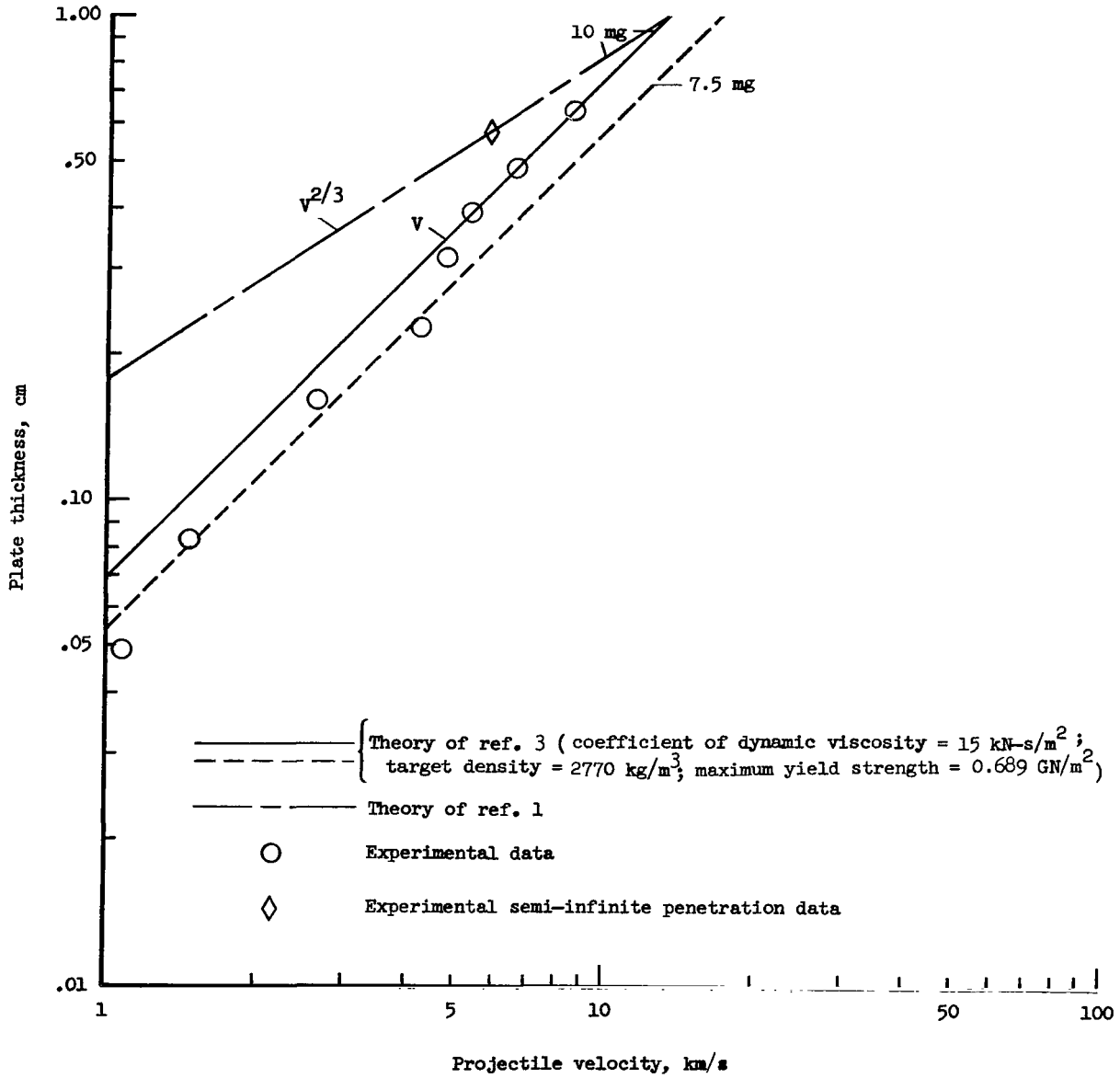

Figure 6.- Ballistic limit velocities for single-sheet 2024-T3 aluminum-alloy targets impacted by 6.4-mm-diameter plastic disks of 10-mg nominal mass.

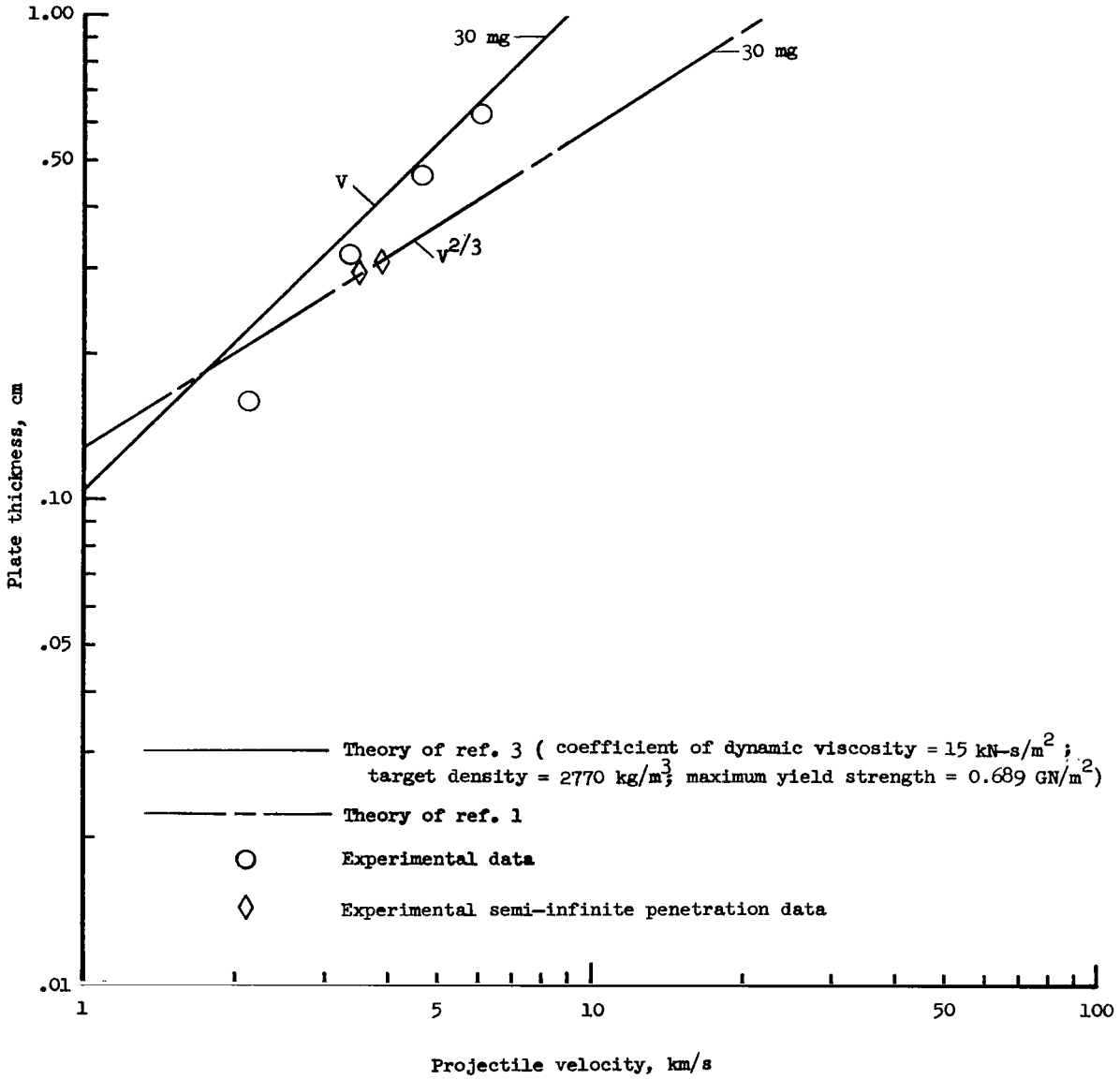

Figure 7.- Ballistic limit velocities for single-sheet 2024-T3 aluminum-alloy targets impacted by 9.5-mm-diameter plastic disks of 30-mg nominal mass.

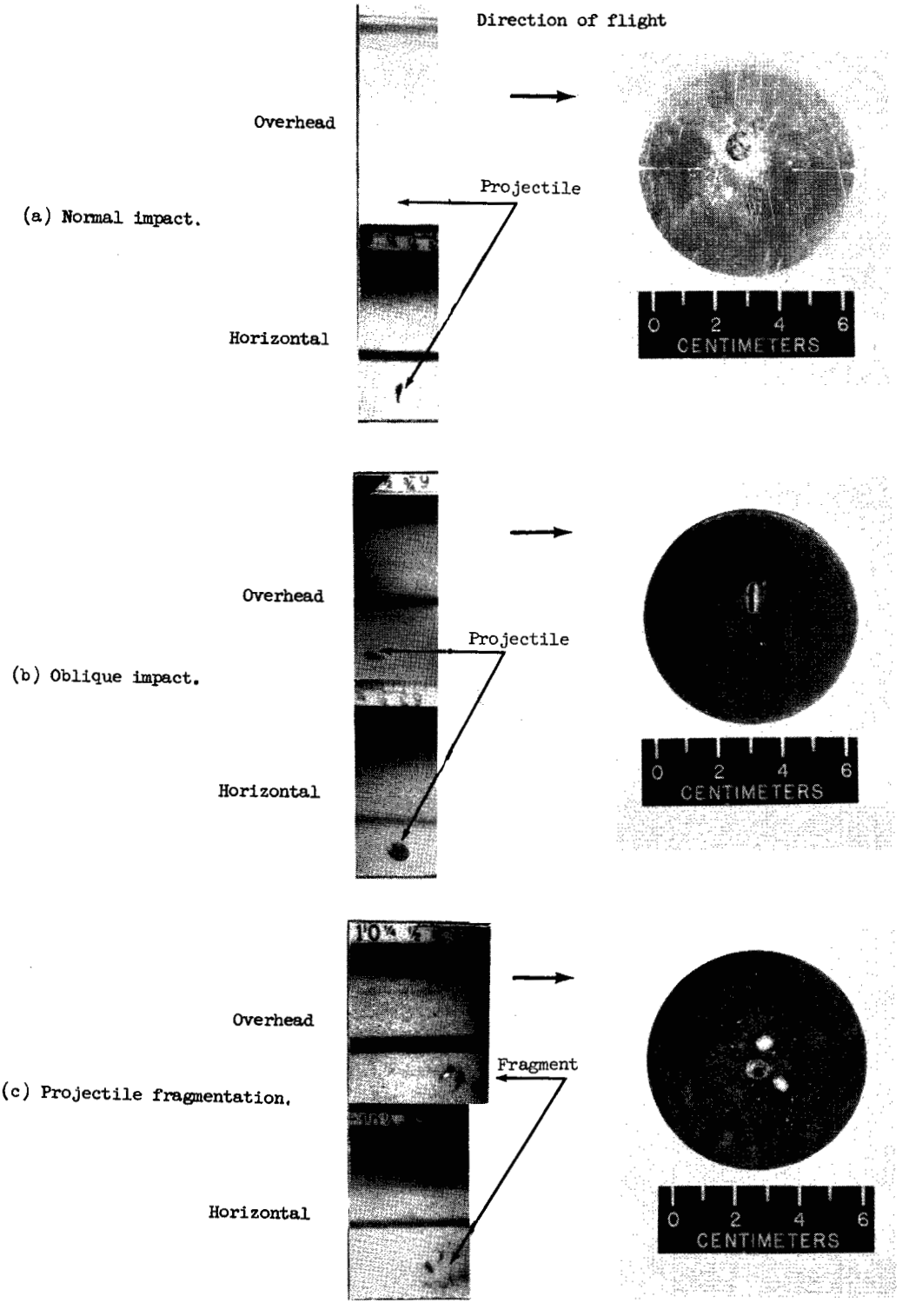

Figure 8.- Modes of projectile impact.

L-67-6656

Comparison of Experiment With Theory

In figures 6 and 7 the experimental ballistic limit velocities for single-plate 2024-T3 aluminum-alloy targets are presented in terms of target plate thickness. Theoretical data are also shown as solid, dashed, and long-short dashed curves. In figure 6 the solid curve is for an impacting disk of 10 mg and the dashed curve for an impacting disk of 7.5 mg. The dashed curve represents the lower limit on projectile mass for an acceptable data point. In figure 7 the solid curve is for a projectile mass of 30 mg. The solid and dashed curves are determined from the theory of reference 3, in which the coefficient of dynamic viscosity, maximum yield strength (shear), and density of the target sheet material were assumed to have values of 15 kN-s/m^2 (1 kN-s/m^2 = 10^4 poise), 0.689 GN/m^2 (1 GN/m^2 = 145 ksi), and 2770 kg/m^3, respectively. Note that a definite correspondence between the slope of the solid curve and the experimental data is established, as shown in both figures 6 and 7. It follows then that the dependence of the ballistic limit on plate thickness is linear. The experimental data as given in figure 6 are essentially bracketed between the solid and the dashed curves and indicate that, although the mass determination for each experimental point is not exactly known, the aggregated results show a definite correspondence with the theoretical results of reference 3. It is noteworthy that a linear dependence between target-plate thickness and ballistic limit has also been established experimentally by Fish and Summers (ref. 7) for spherical projectiles. It should be noted, however, that the treatment of thin-plate perforation in reference 3 is a one-dimensional analysis in which it is assumed that a thin disk is the impacting projectile, and the application of this analysis to spherical projectiles must necessitate the inclusion of two-dimensional effects.

The long-short dashed curve represents the ballistic limit target-plate-thickness dependence of 1.5 times the depth of penetration into a semi-infinite target at hypervelocities. (See refs. 1, 2, 8, and 9.) This curve has been positioned by use of an experimentally determined semi-infinite penetration data point for disks impacting on thick 2024-T3 aluminum-alloy plates. It was given a constant slope of two-thirds (ref. 1) on the log-log scale and is shown in figures 6 and 7 for comparison purposes only. The experimental data do not follow the ballistic limit target-plate-thickness dependence of velocity raised to the two-thirds power $V^{2/3}$ as can be seen from figures 6 and 7.

CONCLUDING REMARKS

The experimental ballistic limit data presented in this program correlates well with the theory of ballistic limit developed from a visco-plastic model. The ballistic limit plate-thickness dependence is shown experimentally to follow the linear relation predicted from visco-plastic theory. Consequently, the concept of correlating the ballistic limit of

finite plates to cratering depth in semi-infinite targets at hypervelocities is invalid. Hence, experimental data obtained in the penetration of semi-infinite targets are not applicable in predicting the ballistic limits of thin plates and should not be used in describing finite plate behavior.

An exploding foil gun facility at the Langley Research Center has produced reliable and consistent ballistic limit data. Certain precautions must be observed, however, in evaluating data obtained with this gun, such as loss in projectile mass and projectile orientation at impact. By careful calibration, compensation, and selection of acceptable shots, the exploding foil gun has been found to be a useful tool for ballistic limit measurements. The gun has demonstrated its flexibility in varying the projectile velocity and mass and, in particular, its ability to fire a large number of low cost test shots within a short time interval.

Langley Research Center,
National Aeronautics and Space Administration,
Langley Station, Hampton, Va., June 21, 1967,
124-08-01-13-23.

REFERENCES

1. Christman, D. R.: Target Strength and Hypervelocity Impact. AIAA J. (Tech. Notes), vol. 4, no. 10, Oct. 1966, pp. 1872-1874.

2. Herrmann, Walter; and Jones, Arfon H.: Survey of Hypervelocity Impact Information. A.S.R.L. Rept. 99-1, Massachusetts Inst. Technol., Sept. 1961. (Available from ASTIA as Doc. AD 267 289.)

3. Thomson, Robert G.; and Kruszewski, E. T.: Effect of Target Material Yield Strength on Hypervelocity Perforation and Ballistic Limit. Proceedings of the Seventh Hypervelocity Impact Symposium, vol. V, Feb. 1965, pp. 273-320. (Sponsored by U.S. Army, U.S. Air Force, and U.S. Navy.)

4. Mechtly, E. A.: The International System of Units – Physical Constants and Conversion Factors. NASA SP-7012, 1964.

5. Anon.: Mylar – Physical, Electrical, and Chemical Properties. Tech. Rept. TR-1, E. I. Du Pont de Nemours & Co., Inc.

6. Scherrer, Victor E.: An Exploding Wire Hypervelocity Projector. Exploding Wires, Volume 2, William G. Chace and Howard K. Moore, eds., Plenum Press, 1962, pp. 235-244.

7. Fish, Richard H.; and Summers, James L.: The Effect of Material Properties on Threshold Penetration. Proceedings of the Seventh Hypervelocity Impact Symposium, vol. VI, Feb. 1965, pp. 1-26. (Sponsored by U.S. Army, U.S. Air Force, and U.S. Navy.)

8. Andriankin, É. I.; and Stepanov, Yu. S.: Impact Penetration Depth of Meteoric Particles. Artificial Earth Satellites, vol. 15, Jan. 1964, pp. 45-53.

9. Kinard, William H.; Lambert, C. H. Jr.; Schryer, David; and Casey, Francis W., Jr.: Effect of Target Thickness on Cratering and Penetration of Projectiles Impacting at Velocities to 13,000 Feet Per Second. NASA MEMO 10-18-58L, 1958.

TABLE I.- EXPERIMENTAL BALLISTIC LIMITS FOR SINGLE-SHEET 2024-T3 ALUMINUM-ALLOY TARGETS IMPACTED BY DISKS

Experimental ballistic limit, km/s (a)	Sheet thickness, mm
Diameter, 6.4 mm; nominal mass, 10 mg	
1.08	0.48
1.46	.83
2.62	1.61
4.23	2.28
4.72	3.25
5.18	3.94
6.25	4.85
8.47	6.35
Diameter, 9.52 mm; nominal mass, 30 mg	
2.13	1.61
3.35	3.25
4.63	4.76
6.05	6.35

[a]Obtained by bracketing the ballistic limit from a series of experimental shots.

NASA-Langley, 1967 —— 32 L-5153

"The aeronautical and space activities of the United States shall be conducted so as to contribute . . . to the expansion of human knowledge of phenomena in the atmosphere and space. The Administration shall provide for the widest practicable and appropriate dissemination of information concerning its activities and the results thereof."

—NATIONAL AERONAUTICS AND SPACE ACT OF 1958

NASA SCIENTIFIC AND TECHNICAL PUBLICATIONS

TECHNICAL REPORTS: Scientific and technical information considered important, complete, and a lasting contribution to existing knowledge.

TECHNICAL NOTES: Information less broad in scope but nevertheless of importance as a contribution to existing knowledge.

TECHNICAL MEMORANDUMS: Information receiving limited distribution because of preliminary data, security classification, or other reasons.

CONTRACTOR REPORTS: Scientific and technical information generated under a NASA contract or grant and considered an important contribution to existing knowledge.

TECHNICAL TRANSLATIONS: Information published in a foreign language considered to merit NASA distribution in English.

SPECIAL PUBLICATIONS: Information derived from or of value to NASA activities. Publications include conference proceedings, monographs, data compilations, handbooks, sourcebooks, and special bibliographies.

TECHNOLOGY UTILIZATION PUBLICATIONS: Information on technology used by NASA that may be of particular interest in commercial and other non-aerospace applications. Publications include Tech Briefs, Technology Utilization Reports and Notes, and Technology Surveys.

Details on the availability of these publications may be obtained from:

SCIENTIFIC AND TECHNICAL INFORMATION DIVISION

NATIONAL AERONAUTICS AND SPACE ADMINISTRATION

Washington, D.C. 20546